AN EXPERIMENTAL EVALUATION OF THEORY FOR DIFFUSION CONTROLLED COULOSTATIC RELAXATION

Thesis for the Degree of M. S.
MICHIGAN STATE UNIVERSITY

Frank Matthew Michaels

1970

ABSTRACT

AN EXPERIMENTAL EVALUATION OF THEORY FOR DIFFUSION CONTROLLED COULOSTATIC RELAXATION

Previously, experimental applications of the coulostatic technique have been limited to perturbations from equilibrium of less than 4/n mV, because of assumptions in the derivation of the theoretical equations. Recent theoretical studies, however, have indicated that perturbations as large as 25/n mV should yield the same results as the previous small perturbation theory when the normalized relaxation curves are compared. In this work an attempt was made to test these predictions experimentally for the case of diffusion controlled relaxation. Thus, the ferrous-ferric oxalate couple, which is known to have a large electron transfer rate constant, was investigated by the coulostatic method. Normalized relaxation curves for perturbations ranging from 7 to 43 mV from equilibrium were recorded and compared with the small perturbation theory. A profound lack of agreement was found between the theory and experimental results even for small perturbations from equilibrium. In an effort to determine the source of this disagreement between theory and experiment, each of the assumptions of the theoretical model was

tested experimentally, but no discrepancies were found which could explain the magnitude of the deviation observed.

AN EXPERIMENTAL EVALUATION OF THEORY FOR DIFFUSION CONTROLLED COULOSTATIC RELAXATION

By

Frank Matthew Michaels

A THESIS

Submitted to
Michigan State University
in partial fulfillment of the requirements
for the degree of

MASTER OF SCIENCE

Department of Chemistry

1970

VITA

Name: Frank Matthew Michaels

Born: March 12, 1943, in Cleveland, Ohio

Academic Career: Benedictine High School
Cleveland, Ohio 1957 - 1961

Case Institute of Technology
Cleveland, Ohio 1961 - 1965

Degree Held: B.S. Case Institute of Technology (1965)

ACKNOWLEDGEMENT

The author wishes to convey his sincere appreciation to Professor Richard S. Nicholson for his guidance and encouragement in the course of this work.

The author also wishes to thank Professor C. G. Enke for permitting the use of some of his research equipment during this study.

TABLE OF CONTENTS

	Page
INTRODUCTION	1
THEORY	8
Model	8
Results	9
EXPERIMENTAL	12
Selection of a Chemical System	12
Instrumentation for Coulostatic Experiments	14
Circuit of Delahay	14
Circuit of Lauer	16
Circuit of Daum and Enke	19
Measurement of Double Layer Capacitance	28
Cell and Electrodes	28
Chemicals	29
Procedures	29
RESULTS AND DISCUSSION	31
Low Overpotential Experiments	31
Effect of Electron Transfer Kinetics	32
Errors in τ_O and τ_R	35
Effect of Finite Current Injection Time	39
Errors in ΔE_i	40
Other Sources of Error	41
Effect of Large Overpotentials	42

TABLE

TABLE		Page
I.	Comparison of Relaxation Curves for Large and Small Overpotentials	11

LIST OF FIGURES

FIGURE		Page
1.	Diagram of the circuit due to Delahay.	4
2.	Circuit Diagram of the semiconductor switch. . .	18
3.	Diagram of the circuit due to Lauer.	21
4.	Equivalent circuit for the cell.	24
5.	IR compensator and final circuit configuration .	27
6.	Comparison of theoretical and experimental relaxation curves.	34
7.	Stationary electrode polarogram for supporting electrolyte without depolarizer.	38
8.	Relaxation curves for larger perturbations from equilibrium on the ferrous-ferric oxalate system	44

INTRODUCTION

The use of relaxation methods to study the rates of fast homogeneous chemical reactions is fairly commonplace. Generally, with these methods the equilibrium state of a chemical system is perturbed by abruptly changing one of the variables defining that equilibrium state. The rate of return (relaxation) of the system to equilibrium is determined by chemical reaction rates, and therefore can be used to measure rate constants.

The coulostatic technique[1,2] can be thought of as an application of these ideas to the study of heterogeneous electrochemical reactions. In the initial equilibrium state the electrode potential is determined by the concentration of depolarizer at the electrode surface through the Nernst equation. This equilibrium potential is then rapidly perturbed by altering the charge in the electrical double layer of the electrode. This rapid injection of charge can be accomplished in several ways, the simplest being the circuit of Figure 1 — (this circuit was first used by Delahay[3] in his initial investigations of the coulostatic technique). Initially, capacitor, C, is charged by battery, B. Switch, S, is then thrown to charge the electrical double layer. By

having C small with respect to the double-layer capacitance, the discharge of C can take place in a very short time. The electrode potential reached at the end of the coulostatic impulse is

$$E = E_{eq} + \frac{q}{C} \qquad (1)$$

Figure 1. Diagram of the Circuit Due to Delahay.[3]

A: Cell

B: Battery

C: Capacitor

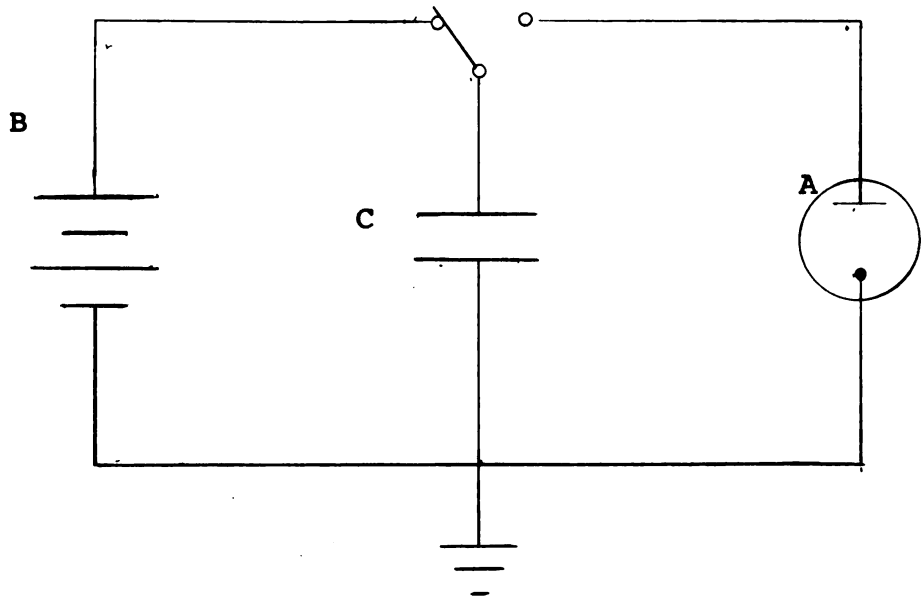

Figure 1

where E_{eq} is the initial equilibrium potential, q is the coulombic charge injected, and C is the double layer capacitance.

Since the new electrode potential, E, does not correspond to the equilibrium concentration of depolarizer, Faradaic reaction takes place, discharging the double-layer. As the double layer is discharged, the electrode potential relaxes back toward the initial potential, E_{eq}. Initially, the extent of Faradaic reaction is governed by the rate of the electron transfer reaction, and therefore the relaxation is kinetically controlled. As the Faradaic reaction proceeds, however, concentration gradients develop near the electrode surface and the mass transport process (usually diffusion) also determines the rate of relaxation. Thus, theory for the coulostatic method must consider both diffusion and electron transfer kinetics. For a first order electrode reaction, the rate of electron transfer is given by the following well known equation[4]:

$$i_f = nFAk_s (C_O^*)^{1-\alpha} (C_R^*)^{\alpha} \left\{ \frac{C_O}{C_O^*} \exp\left(-\frac{\alpha n F}{RT}\eta\right) - \frac{C_R}{C_R^*} \exp\left[(1-\alpha)\frac{nF}{RT}\eta\right] \right\} \quad (2)$$

where i_f is the faradaic current

α = transmission coefficient

k_s = standard electrochemical rate constant

η = overpotential

C_R, C_O = surface concentrations of reduced and oxidized species

C_R^*, C_O^* = bulk concentrations of reduced and oxidized species

The other parameters have their usual meaning.

When diffusion also must be considered, Equation 2 constitutes a boundary condition for solution of the Fick diffusion equations. Because the relationship between potential and concentration in Equation 2 is nonlinear, in general the Fick boundary value problem cannot be solved analytically. Thus it is common practice to linearize Equation 2 by expanding the exponentials in a Taylor series and retaining only the first two terms. For this approximation to be valid at the 1% error level the argument of the exponentials must be less than 0.15. In terms of Equation 2 this condition corresponds to potential excursions less than 3/N mV. From an experimental point of view the use of such

small overpotentials is difficult when signal to noise ratios are considered. Actually, it is conceivable that the exponential terms are of minor importance in the final result, so that larger overpotentials could be used without increasing the above error level. In the case of purely diffusional relaxation this appears to be so. Nicholson[5] has solved the boundary value problem without introducing linearization, and found that results agree with linearized theory for overpotentials as large as 25/n mV. Since this fact has important implications in terms of electrochemical relaxation methods, it was decided to test experimentally the theory published by Nicholson. The results are described in the remainder of this thesis.

THEORY

For an experimental evaluation of coulostatic theory to be meaningful it is important to carefully define the theoretical model. The model assumed by Nicholson and in most other treatments of coulostatic relaxation is therefore described next.

Model. The following major assumptions were used by Nicholson in developing a theoretical description of coulostatic relaxation:

1. Mass transport occurs by linear diffusion. This implies the absence of convection or electrical migration affecting the electroactive species, and assumes that a planar electrode is employed.
2. The concentration of depolarizer in the bulk of solution remains unchanged within the time scale of the experiment.
3. No adsorption or other accumulation occurs at the electrode surface.
4. The injection of charge is instantaneous.

5. The double layer capacitance is independent of potential over the potential range of the experiment.
6. The potential relaxation is diffusion controlled at all times. This means that the electrochemical rate constants are large enough that the Nernst equation concentrations are always maintained at the electrode surface even immediately after the initial impulse. The rate of potential decay will then be determined by the rate of diffusion of electroactive species to the surface.

Results. The above model can be expressed mathematically as the following nonlinear integral equation first derived by Nicholson[5].

$$\Psi_i \, 2\sqrt{t/\tau_O} - \int_0^{t/\tau_O} \frac{\Psi(\xi)\,d\xi}{\sqrt{t/\tau_O - \xi}} = \int_0^{t/\tau_O} \frac{\exp[\Psi(\xi)] - 1}{1 + \sqrt{\tau_R/\tau_O}\,\exp[\Psi(\xi)]}\,d\xi \qquad (3)$$

The following definitions apply to Equation (3)

$$\Psi(t) = \frac{nF}{RT}\,\Delta E(t) \qquad (4)$$

$$\Psi_i = \frac{nF}{RT}\,\Delta E_i \qquad (5)$$

$$\tau_O^{\frac{1}{2}} = \frac{RT}{n^2F^2}\frac{C}{A}\frac{1}{\sqrt{\pi D_O}\, C_O^*} \qquad (6)$$

$$\tau_R^{\frac{1}{2}} = \frac{RT}{n^2F^2}\frac{C}{A}\frac{1}{\sqrt{\pi D_R}\, C_R^*} \qquad (7)$$

There $\Delta E(t)$ is the electrode potential as a function of time; ΔE_i is the initial potential displacement from equilibrium, C is the differential double layer capacitance, A is the electrode area, D_O and D_R are diffusion coefficients for the oxidized and reduced forms of the depolarizer, C_O^* and C_R^* are initial bulk concentrations of depolarizer, and other terms have their usual meaning. Thus, the function $\Psi(t)$, which is the solution of Equation 3, directly gives the potential - time relaxation for any initial perturbation, Ψ_i. The solution of Equation 3, and hence the rate of relaxation, is determined by the two diffusional relaxation constants, τ_O and τ_R.

Equation 3 is nonlinear because of the exponential terms, and therefore Equation 3 cannot be solved analytically. If potential excursions are restricted to less than 3/n mV, however, the exponential terms can be expanded as a truncated Taylor

series in which only first order terms are retained. This results in the following solution obtained first by Reinmuth.[6]

$$\Psi(t) = \Psi_i \exp\left[t/\pi(\sqrt{\tau_O} + \sqrt{\tau_R})^2\right] \operatorname{erfc}\left[\sqrt{t}/\sqrt{\pi}(\sqrt{\tau_O} + \sqrt{\tau_R})\right] \quad (8)$$

all terms in Equation 8 have been defined previously.

Equation 3 was solved numerically by Nicholson for various perturbations from equilibrium. The results of solving Equation 3 for a 25/n mV, perturbation are listed in Table I along with data calculated from Equation 8. A comparison of the two sets of data shows that they agree within 2% . Thus these theoretical data indicate that some of the errors introduced by the linearization tend to cancel, so that larger perturbations can be used in the coulostatic technique while the data can still be interpreted in a straightforward manner using Equation 8.

Table I. Comparison of Relaxation Curves for Large and Small Overpotentials

t/τ_o	ψ/ψ_i [a]	ψ/ψ_i [b]
.01	.969	.977
.05	.933	.940
.10	.907	.915
.50	.809	.819
1.0	.747	.758
5.0	.554	.563
10.	.458	.466
50.	.256	.259

[a] Linearized theory from Equation 8.

[b] Nonlinearized theory from Equation 3; data are for $\psi_i = 25/n$ mV.

EXPERIMENTAL

Selection of a Chemical System

Success in comparing theory with experiment is dependent on how faithfully the theoretical model describes the experimental conditions. Some assumptions of the model are satisfied without difficulty, while others are impossible to achieve vigorously. Thus, the discussion that follows considers each point of the model in terms of selection of experimental conditions and a depolarizer.

The linear diffusion and constant bulk concentration requirements - the so called semi-infinite linear diffusion assumption - is a common constraint in electrochemistry, particularly polarography. This assumption is realized experimentally through use of excess supporting electrolyte to insure mass transport by diffusion, and measurement times less than 1 second to insure linear diffusion.

Adsorption effects would make it impossible to determine the initial concentrations for the experiment. Also, preferential accumulations of the electroactive species at the surface during the experiment would affect the potential - time curves

to an indeterminate degree. These problems can be averted by selecting a depolarizer for which adsorption phenomena are known to be absent as indicated by other electrochemical techniques. Since only small overpotentials are used in coulostatic experiments, the variation of double layer capacitance with potential is usually negligible over these relatively small potential ranges. The double layer itself is almost entirely composed of ions of the supporting electrolyte, because of the large excess of electrolyte with respect to the concentration of depolarizer. The double layer capacitance therefore, can be measured as a function of potential by performing cyclic voltammetry experiments on the inert electrolyte.

The model assumes that Nernstian conditions are maintained during the entire experiment, a condition which is clearly impossible to achieve vigorously since it would require an infinitely large electron transfer rate constant. Nevertheless, by using a depolarizer for which the electron transfer rate constant is very large (greater than 1 cm/sec.), deviations from Nernstian behavior can be limited to the first few microseconds of the relaxation. In addition, by employing relatively low concentrations of depolarizer, onset of diffusion control can be hastened.

To summarize, in terms of the model the major requirements for a chemical system are; large electron transfer rate constant, absence of adsorption, and both forms of the redox couple soluble in the solution phase. An examination of the electrochemical literature revealed that the ferrous - ferric oxalate couple in 0.15 M binoxalate satisfies these criteria [e.g. k_s > 1 cm/sec [7]], and therefore this system was selected for evaluation of the theoretical calculations.

The only point of the model not yet discussed is Point 4, the assumption that the coulombic charge injection can be accomplished in an infinitesimally small time. This condition, of course, can never be realized experimentally, since it would require an infinite current from the potential source. Nevertheless, with suitable instrumentation the charge injection can be accomplished in a very short time. A number of different approaches are possible, and several of these were evaluated as a part of this investigation. The results of this study, as well as a description of the circuit actually used to collect data reported in this thesis, are presented next.

Instrumentation for Coulostatic Experiments

Circuit of Delahay.[3] The circuit of Figure 1, due to Delahay, although simple in principle, cannot be used directly

since the mechanical switching operations introduce large spikes and spurious noise which take up to 100 μ sec. to decay. It would seem that the switching could be done electronically, however, and this possibility was tested using a commercial SPDT electronic switch (Crystallonics Model CAG7) to duplicate the function of the switch in Delahay's circuit. Since contacts are not formed or broken in this type of switch, the noise problems are eliminated. The CAG7 has a 1.5 μ sec. turn on time with a 6Ω on resistance and a 100ma current capability. The circuit for the switch is shown in Figure 2. Briefly, its operation is as follows. With a logic level of + 5 V, transistor T_1 is maintained in the off state. Point P is then negative, diode D_1 conducts but the field effect transistor (FET) F_1 is reverse biased and is in the off state, so that the cell is effectively out of the circuit. Transistor T_2 is also off, keeping point Q at + 15 V. Since diode D_2 is reversed biased, FET F_2 is on and the capacitor is charged by the battery. When the "logic in" level is switched to 0 (ground), both transistors are on and now F_1 is on while F_2 is off so that the capacitor discharges across the cell. The resistor across the

capacitor is used to provide proper bias for the FET's. The resistor was chosen to be small enough to bias the FET's, yet large enough not to contribute significantly to the discharge of the capacitor across the cell.

Unfortunately it was found with the above circuit that the cell was always biased by a small voltage during the experiment, corresponding to a net current flowing through the cell during the decay. The source of this current was the fact that the diode D_1, though reversed biased, still had a finite resistance. Thus, the +15V from point P is divided through the diode, the drain to gate resistance, and the cell resistance giving the resulting bias during the decay. No immediate solution to this problem was apparent.

Circuit of Lauer.[8] A circuit published by Lauer was designed to eliminate the switching noise of Delahay's design by putting the cell in the control loop of an operational amplifier. The circuit is given in Figure 3. A square wave is input to the amplifier as shown. Current flows through the feedback loop until capacitor C_A reaches a potential equal in magnitude, though opposite in sign to the input source. Point S is then at virtual ground so no further net current flows.

Figure 2. Circuit Diagram of the semiconductor switch.

T_1, T_2: Transistor

D_1, D_2: Diodes

F_1, F_2: Field Effect Transistors

A: Cell

B: Battery

C: Capacitor

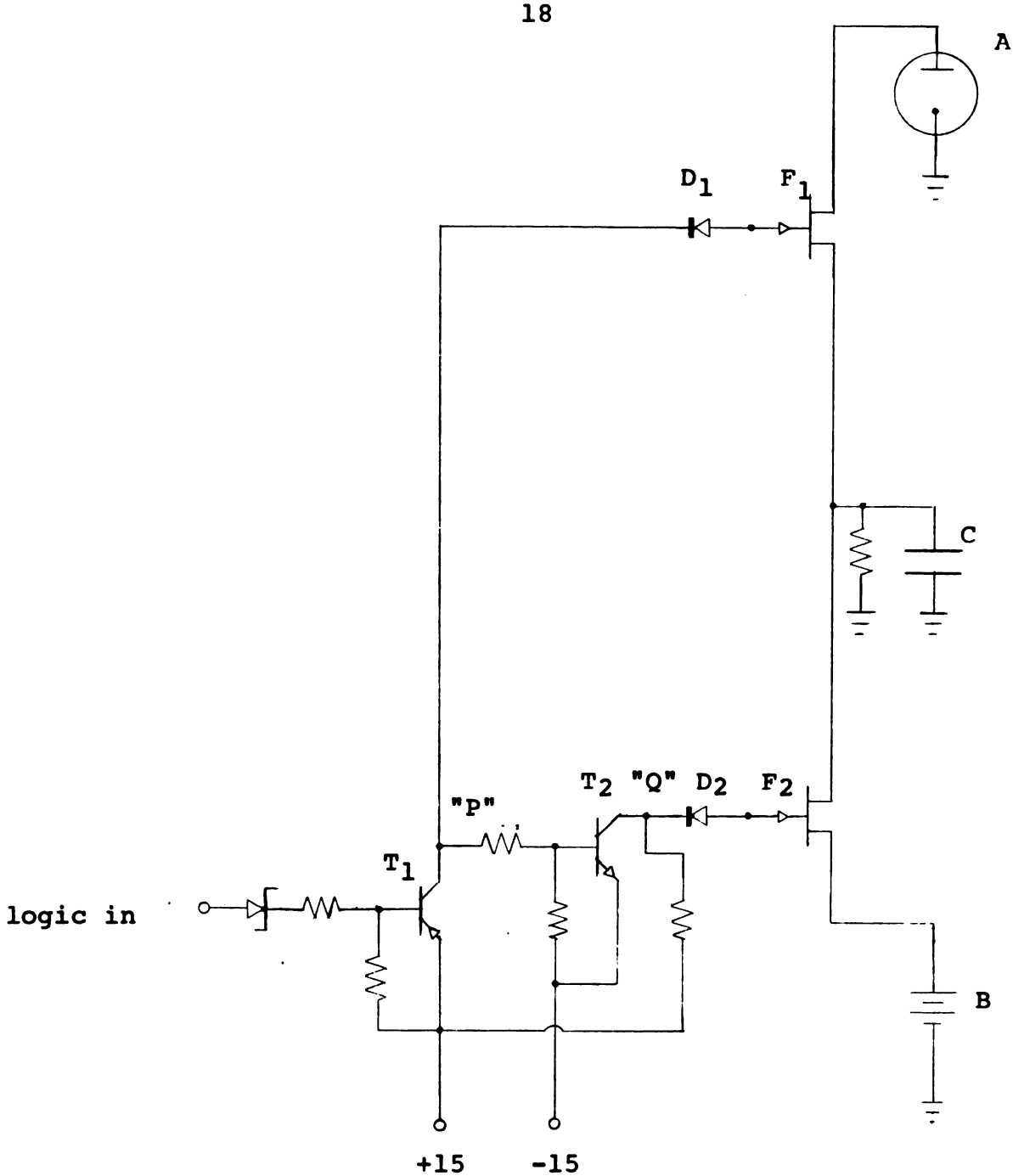

Figure 2

Since all the current which flows through the capacitor also flows through the cell, by knowing the capacitance of C_A, the number of coulombs input to the cell can be calculated. The initial potential can then be determined if the double layer capacitance is known.

Although Lauer claims to have obtained good results with this circuit, when it was constructed in this laboratory considerable difficulty was encountered in terms of maintaining stability. Thus, in order to insure stability, response time had to be sacrificed so that under the best conditions 50 μ sec. were required to charge the cell, which is at least an order of magnitude too large to be useful.

Circuit of Daum and Enke.[9] A commercial current pulse generator (Intercontinental Instruments Incorporated model PG-33) has been used by Daum and Enke to give fast charging without the noise problems obtained with Delahay's circuit. With this instrument the pulse duration can be controlled from 30 n sec. to 2 sec., and the magnitude of the current from zero to 200 ma. The use of a constant current source has a further advantage in that the double layer capacitance can be measured during the changing pulse as described by Wier and

Figure 3. Diagram of the circuit due to Lauer.[8]

G: Square wave pulse generator

R's: Resistors of equal value

oA: Operational amplifier

A: Cell

C: Capacitor

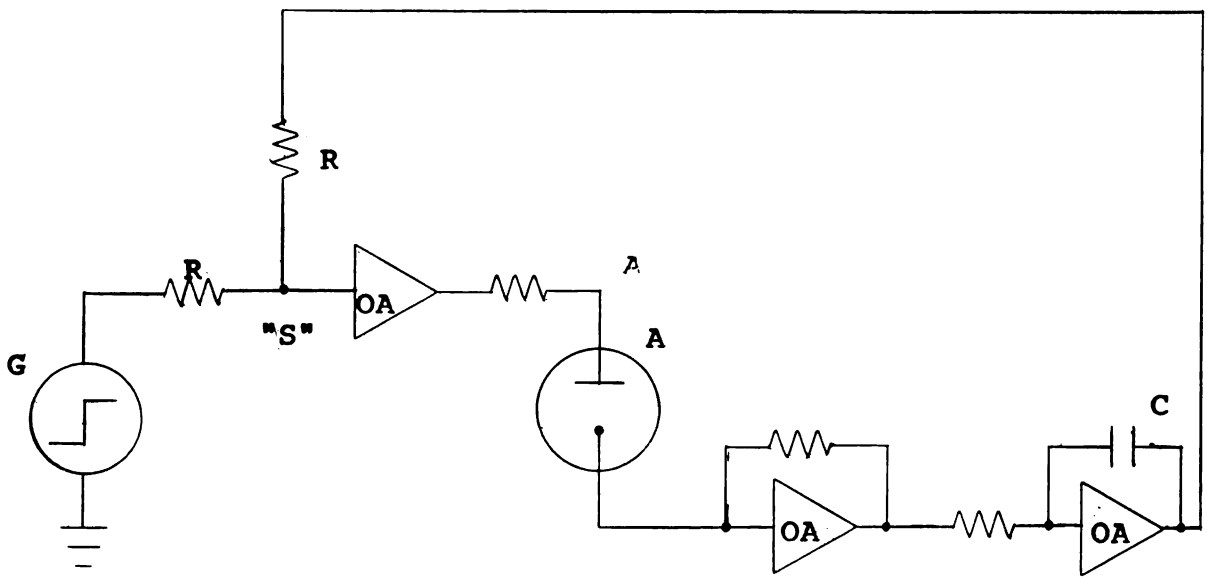

Figure 3

Enke.[10] The equivalent circuit of the cell for the charging process is shown in Figure 4. The magnitude of the constant current, i_p, is given by the differential equation

$$i_p = C \frac{d\Delta E}{dt} + \frac{\Delta E}{R_c} \qquad (9)$$

where ΔE is the potential of the cell without the iR drop due to solution resistance. The solution of Equation 9 is

$$\Delta E = i_p R_C \left(1 - e^{-t/R_c C}\right) \qquad (10)$$

During charging the potential measured, ξ, includes the solution resistance,

$$\xi = i_p R_e + \Delta E \qquad (11)$$

so that the slope of the observed charging curve is

$$\frac{d\xi}{dt} = \frac{d\Delta E}{dt} = \frac{i_p}{C} e^{-t/R_c C} \qquad (12)$$

For measurement times much smaller than the time constant $R_c C$, the slope will equal i_p/C. A typical time constant for these experiments is approximately 5 μ sec.

During the charging pulse relatively large currents are flowing through the cell and and appreciable IR drop, as large as 8V, can be developed across the cell during the current pulse. With the oscilloscope at the high sensitivity required to observe the relaxation curve (e.g. 5mV/div.), saturation of

Figure 4. Equivalent circuit for the cell

R_e: Electrolyte resistance

R_c: Charge transfer resistance

C : Double layer capacitance

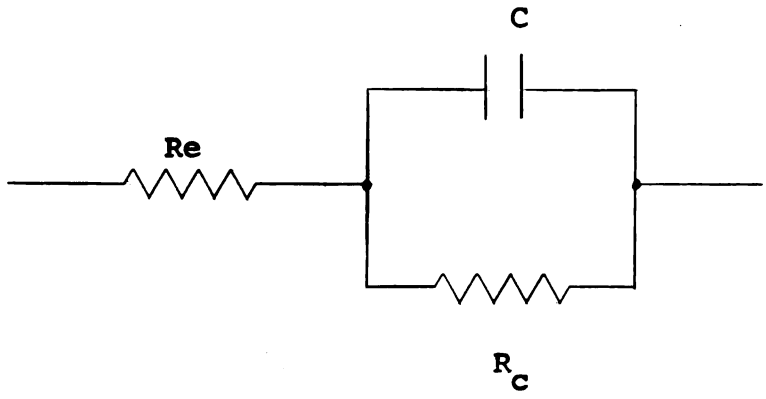

Figure 4

the oscilloscope's input amplifier occurs. These amplifiers recover from saturation fairly slowly, thereby obscuring the initial portion of the relaxation curve. To avoid this problem Daum[11] devised an IR compensator, in which a variable resistor simulates the cell resistance. The current is divided into two branches, one path through this dummy cell, the other through the real cell. By measuring the potential between the resistor and the cell differentially, IR drop across the cell is cancelled, and saturation of the oscilloscope amplifiers prevented. This approach is illustrated in Figure 5. In this figure CPG denotes the current pulse generator, the output of which is divided by matched diodes. Approximately half of the current flows through a resistor which simulates the cell resistance, and whose value can be adjusted with potentiometer P. The other half of the current flows through the cell. The potential is measured differentially between the cell and dummy cell via the oscilloscope. The oscilloscope used was a Tektronix Model 535A with Type W plug in high gain differential amplifier and delayed trigger (T in Figure 5). The net current through the cell was measured between points M and Q across the precision resistor R. All

Figure 5. IR compensator and final circuit configuration

CPG: Current Pulse Generator

R's: Precision resistors of equal value

A : Cell

P : Potentiometer

W : Differential amplifier plug in unit

T : Delayed trigger

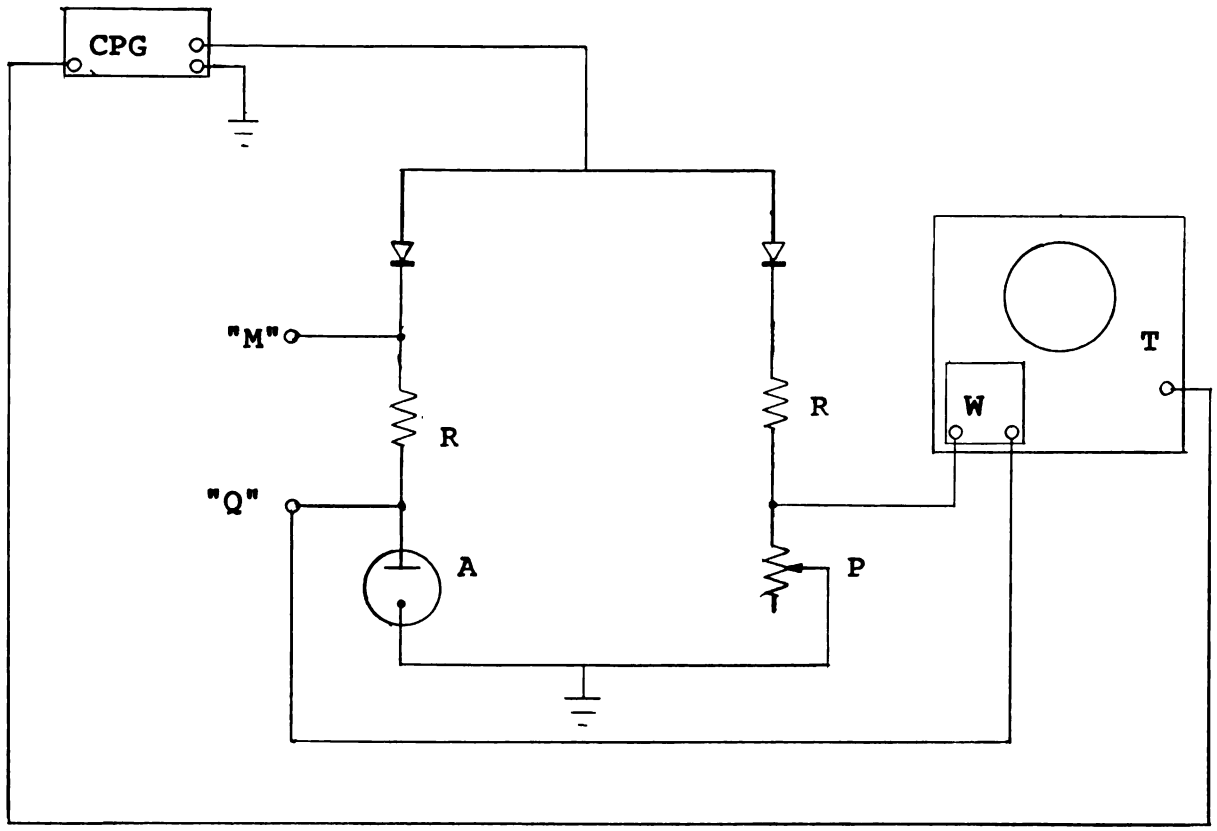

Figure 5

oscilloscope traces were photographed using a Tektronix Type C-12 camera and Model 100 projected graticule.

Measurement of Double Layer Capacitance. The double layer capacitance as a function of potential was determined with cyclic voltammetry on a solution of supporting electrolyte without depolarizer. Double layer capacitance was calculated from the equation

$$C = \frac{i}{dE/dt} \qquad (13)$$

where C is the capacitance at potential E, dE/dt is the scan rate and i is the observed current. These curves were recorded with a three electrode potentiostat (Wenking Potentiostat Model 61 RS) and a commercial function generator (exact, Type 255 s). The same equipment was used in a polargraphic configuration to measure the concentrations of depolarizer.

Cell and Electrodes

For the coulostatic work a two electrode cell configuration was used. The working electrode was a hanging mercury drop. The counter - reference electrode was a mercury plated platinum gauge with area much greater than the working electrode. The geometry of the cell is similar to that described by Wier and

Enke[12] with the gauze surrounding and concentric with the working electrode to minimize noise.

The cell and electrode system used for the cyclic voltammetry and polarographic work were of conventional design and are described elsewhere.[12]

Chemicals.

All chemicals were reagent grade and used without further purification. Argon was saturated over water and passed into the cell to purge the system of dissolved oxygen.

Procedures.

Experiments were performed for various perturbations from equilibrium ranging from 7 mV to 50 mV. For each experiment the charging curve was measured to calculate the double layer capacitance. The current through the cell and charging pulse duration measured via the 100 Ω precision resistor in series with the cell were also recorded for each experiment.

Ammonium sulfate salts were used to introduce the ferrous and ferric ions in approximately equimolar concentrations ($\sim 2 \times 10^{-4}$M). The salts were weighed out on an analytical balance and the concentration checked polarographically.

A 0.15M oxalate solution, made from potassium bin-oxalate acted as a complexing agent, buffer (pH∿2.5), and supporting electrolyte.

RESULTS AND DISCUSSION

Although the original objectives of this research were to evaluate the use of large overpotential relaxation, it seemed wise initially to evaluate the iron oxalate system using standard low overpotential experiments. As will be seen below, the results of these experiments were such that in fact it was impossible to obtain a meaningful evaluation of the effect of large overpotentials.

Low overpotential experiments

Many experiments were performed with over potentials less than 5mV. These data can be conveniently summarized with a single figure by plotting $\Delta E/\Delta E_i$ *vs.* time, which effectively normalizes the experimental data. A plot of this type is shown as Curve A in Figure 6. Before evaluating the effect of large overpotentials, it seemed advisable to compare the experimental data of Figure 6 with predictions of the low overpotential model. To do this it is necessary to know τ_O and τ_R, because then Equation 8 can be plotted as Ψ/Ψ_i (equivalant to $\Delta E/\Delta E_i$ of Figure 6) *vs.* time. Thus, values of τ_O and τ_R, were calculated from Equations 6 and 7 using experimentally determined values

of C_O, C_R, and double-layer capacitance. The literature value[13] for D_O was used for both D_O and D_R. In view of the fact that three oxalate anions are coordinated to both oxidized and reduced forms of the depolarizer,[14] the assumption of the equality of diffusion coefficients seems to be a reasonable one.

Using these calculated values of τ_O and τ_R, it was then possible to compare the experimental data of Figure 6 with theory. The corresponding theoretical plot is labeled as Curve B in Figure 6. Clearly, from Figure 6 there is an alarming lack of agreement between theory and experiment. A number of different experiments were therefore performed in an attempt to identify the source of this discrepancy; results of these experiments are presented next.

Effect of Electron Transfer Kinetics. It is clear from Figure 6 that the observed relaxation is much slower than predicted by diffusion control. One possibility would therefore appear to be that the relaxation is kinetically controlled rather than diffusion controlled. It is reported in the literature that k_s for the ferric oxalate system is greater than 1 cm/sec. Using this value of k_s and Reinmuth's more general

Figure 6. Comparison of theoretical and experimental relaxation curves.

Curve A: experimental, ferrous-ferric oxalate

Curve B: theoretical assuming diffusion control

Curve C: theoretical with simultaneous kinetic and diffusion control

Parameter: $D_O = D_R = 6.3 \times 10^{-6}$ cm^2/sec

$C_O = .19 \times 10^{-3}$ M

$C_R = .17 \times 10^{-3}$ M

$\Delta E_i = 7$ mV

$K_s = 1$ cm/sec

$C = 30.6 \times 10^{-6}$ f/cm

$n = 1$

$\alpha = .5$

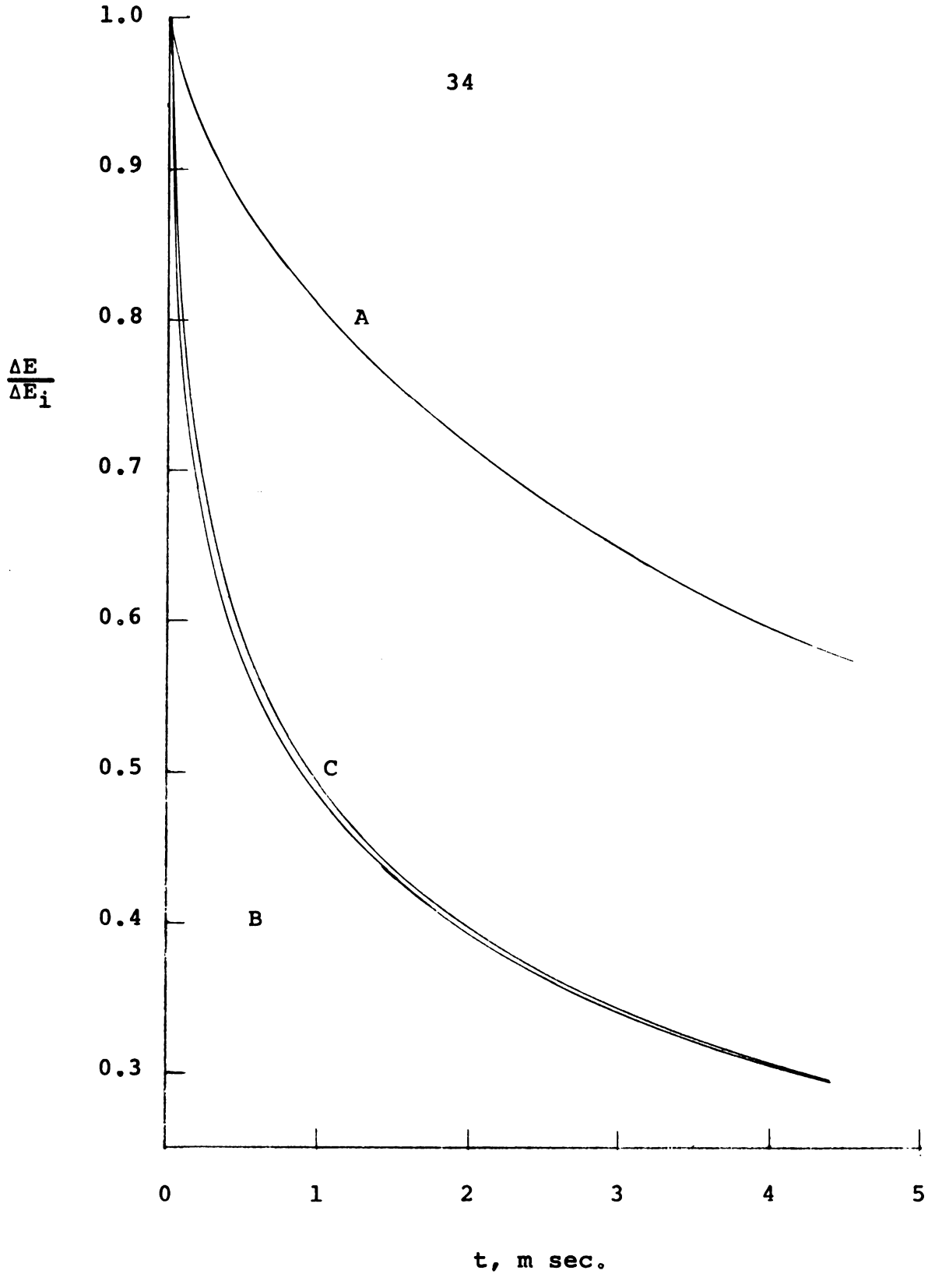

Figure 6

equation[6] for a simultaneous kinetic and diffusion controlled relaxatior, Curve C in Figure 6 is obtained. This curve on the time scale of Figure 6 differs from the diffusion controlled case (Curve B) by only 2%. Thus, either the value of k_s used to calculate Curve C is incorrect, or else the discrepancy cannot be explained by a kinetically controlled relaxation. In fact, to approach the relaxation rate observed experimentally k_s would have to be some three orders of magnitude smaller than the literature value. Independent measurements in this laboratory[15] have shown that this is not the case.

Errors in τ_O and τ_R. Another possible source of the discrepancy between theory and experiment would be large errors in the values of τ_O and τ_R used to calculate the theoretical curve. Since errors in τ_O and τ_R would have to be very large (ca. 90%) to account for the discrepancy, the most likely sources are the bulk concentrations and double layer capacitance, because these quantities are squared in the expressions for τ_O and τ_R. Since the iron oxalate used to prepare solutions was weighed on an analytical balance, and concentrations were checked polarographically, errors in concentration cannot account for the necessary errors in τ_O and τ_R. Nevertheless, double-

layer capacitance was determined by performing coulostatic experiments on blank solutions — i.e., solutions containing only supporting electrolyte. The double layer capacitance was then determined by dividing the number of coulombs by the potential reached in the relaxation. The number of coulombs was determined by recording the potential across the 100 ohm resistor in series with the cell (see Figure 5) and then integrating the resulting current-time curve. An average value of 29.5 $\mu fd/cm^2$ was obtained by this method. Second, to ensure that the presence of depolarizer had no appreciable effect on the double-layer capacitance, the method of measuring the slope of the initial charging curve described earlier was employed. These measurements must necessarily be performed at very short times, where considerable ringing was observed, and therefore these measurements are less precise than those above. Nevertheless, with this method an average value of 28.7 $\mu fd/cm^2$ was obtained. Finally, to determine the potential dependence of the double-layer capacitance, cyclic voltammetry on a blank solution was performed. Typical results are shown in Figure 7. When it is recalled that for this curve double-layer capacitance is simply $i/(dE/dt)$, where dE/dt is constant, it apparent that

Figure 7. Stationary electrode polarogram for supporting electrolyte without depolarizer.

Species: potassium binoxalate

Concentration: .15 M

Scan rate = 165 v/sec

area of electrode = .051 cm^2

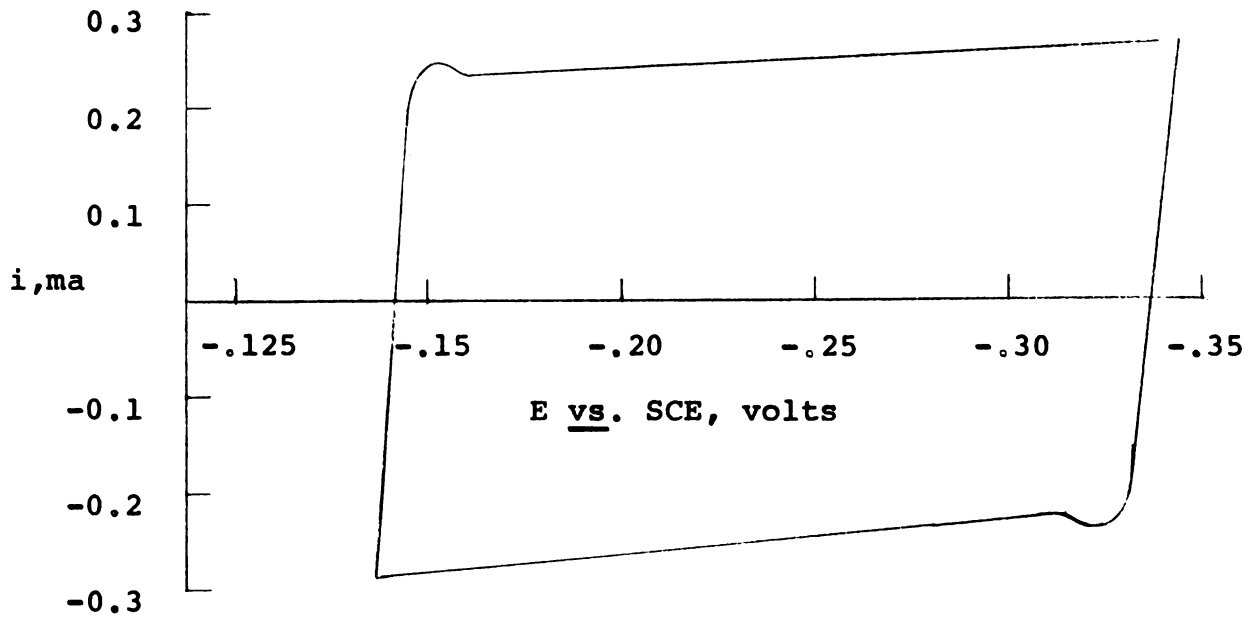

Figure 7

over the small potential range covered in the relaxation experiments, double layer capacitance is constant. The average value of the double layer capacitance calculated from Figure 7 is 30.6 $\mu fd/cm^2$. Thus, the results of all these experiments make it very unlikely that errors in double-layer capacitance can account for large errors in τ_O and τ_R.

Effect of finite current injection time. Theoretically it is assumed that current injection occurs in zero time. Experimentally, this is impossible and therefore the effect of finite injection time was investigated as a possible source of error.

This source of error would apparently describe at least the direction of discrepancy observed between theory and experiment. Thus, if appreciable Faradaic reaction were to take place during the charge injection process, then after cessation of the impulse there would already be some concentration polarization at the electrode surface. This fact would require that depolarizer diffuse to the electrode from further out in the bulk of the solution. This in turn would make the relaxation slower than predicted by the theory, which implicitly assumes the absence of Faradaic reaction during charge injection.

To determine the effect of finite charge injection time, experiments were performed in which the injection time was progressively decreased from 1.0 to 0.1 μ sec. As the injection time was decreased, the amplitude of the current impulse was progressively increased so as to keep the total coulombic content of the pulse constant. The potential time curves were virtually identical for these experiments so that no trend was observed on decreasing the pulse duration. Thus, the effect of finite injection time apparently is not a serious source of error.

Errors in ΔE_i. The only remaining logical source of error is in the parameter ΔE_i, the electrode potential immediately after cessation of the current impulse. Thus, ΔE_i was used in normalizing the experimental data to compare them with theory, so that large errors in ΔE_i could cause the apparent discrepancy between theory and experiment. Unfortunately, ΔE_i could not be measured directly because of ringing observed in the relaxation curves immediately after cessation of the current impulse. Thus, ΔE_i had to be determined by calculating from the equation

$$\Delta E_i = \frac{q}{C} \qquad (13)$$

where q us the change in total coulombic charge in the double-layer following the impulse, and C is double-layer capacitance. Errors in ΔE_i, therefore, could arise either from errors in q and/or C. The total charge injected is accurately known, and therefore the only possible source of error in q is if appreciable charge were consumed by Faradaic reaction during the charge injection. This possibility, however, has already been eliminated (see discussion above concerning finite injection time).

Likewise, experiments described above make it unlikely that errors in C are very large. Finally, although ringing obscured the initial relaxation, values of ΔE_i estimated from photographs of relaxation curves agreed with values of ΔE_i calculated from Equation 13.

Other sources of error. It is believed that the experiments described above cover all logical sources of error. Thus, the only explanation for the large discrepancy between theory and experiment appears to be serious inadequancies in the theoretical model, or previously unknown complications in the electrochemistry of the iron oxalate system. The latter could include coupled chemical reactions or adsorption, either of

which could account for the observed behavior. To invoke specific explanations of this type, however, would be entirely speculative, and serve little purpose at this time.

Effect of Large Overpotentials

The original objectives of this research were to evaluate the effect of large overpotentials on coulostatic relaxation. Obviously, in view of the results reported above, conclusions from large overpotential experiments can not be very meaningful in terms of the original objectives. Nevertheless, some experiments were performed using overpotentials as large as 43 mV. Results of these experiments are summarized in Figure 8. These data show that the rate of relaxation for the iron oxalate system increases with increasing overpotential. This result is contrary both to theory and intuition for electron transfer in an uncomplicated redox couple, and is further evidence that the electrochemistry of iron oxalate is more complex than previously assumed.

Figure 8. Relaxation curves for larger perturbations from equilibrium on the ferrous-ferric oxalate system.

Curve A: relaxation for 7 mV perturbation

Curve B: relaxation for 26 mV perturbation

Curve C: relaxation for 43 mV perturbation

perameters: $C_O = .19 \times 10^{-3}$ M

$C_R = .17 \times 10^{-3}$ M

$C = 30.6 \times 10^{-6}$ f/cm^2

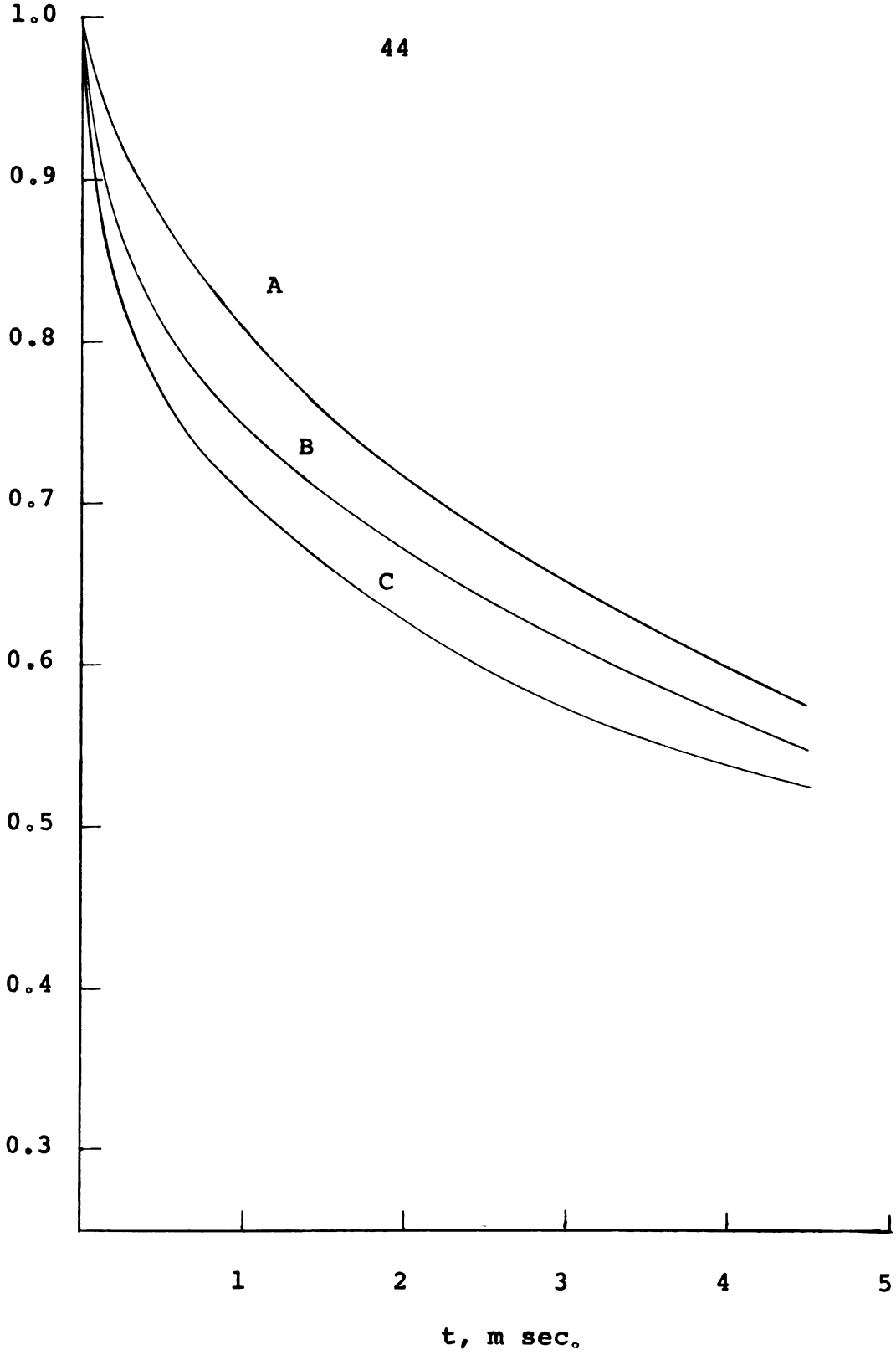

Figure 8

LITERATURE CITED

1. Delahay, P., Anal. Chim. Acta 27, 90 (1962).

2. Reinmuth, W. H., Anal. Chem., 36, 211 R (1964).

3. Delahay, P., Ibid., 34, 1267 (1962).

4. Delahay, P., "New Instrumental Methods in Electrochemistry," Interscience Publishers Inc., New York, N.Y., 1954, P. 35.

5. Nicholson, R. S., Anal. Chem., 37 667 (1965).

6. Reinmuth, W. H., Ibid., 34 1272 (1962).

7. Randles, J. E. B., and Somerton, K. W., Trans. Faraday Soc. 48, 937 (1952).

8. Lauer, G., Anal. Chem., 38, 1277 (1966).

9. Daum, P. H., and Enke, C. G., Ibid., 653 (1969).

10. Weir, W. D., and Enke, C. G., J. Phys. Chem. 71, 275 (1967).

11. Daum, P. H., Ph.D. Dissertation, Michigan State University, 1969.

12. Alberts, G. S., and Shain, I., Anal. Chem., 35, 1859 (1963).

13. Olmstead, M. L., and Nicholson, R. S., Ibid. 38, 150 (1966).

14. Kolthoff, I. M., and Lingane, J. J., "Polarography," Interscience Publishers, Inc., New York, N. Y., 1941, P. 168.

15. Nicholson, R. S., personal communication, 1970.